World's Largest Light-gage Steel Primary Structure

Lev Zetlin

Charles H. J. Thornton

Richard L. Tomasetti

WORLD'S LARGEST LIGHT-GAGE STEEL PRIMARY STRUCTURE

by

Lev Zetlin[1], Ph. D., F. ASCE

Charles H. Thornton[2], Ph. D., A.M. ASCE

and Richard L. Tomasetti[3], A.M. ASCE

I. INTRODUCTION

Two superbay hangars just constructed for the American Airlines Boeing 747's in Los Angeles and San Francisco, indicate the tremendous potential for the use of light-gage steel as primary structure for economical construction. Prior to this time, there has been limited use of cold formed steel sheet as primary structure and it has been essentially unheard of for free form very large span roofs. The light-gage, 230-foot long cantilevered shell roofs of the American Airlines' hangars weigh approximately 40% less than conventional steel construction resulting in substantial cost savings.

The design and economics of buildings requiring clear spans to enclose several enormous aircraft, such as the Boeing 747, the Lockheed L-500, or the Douglas DC-10, has dictated the need for developing completely new concepts for large span structures rather than just using bigger conventional components. The structural system for the American Airlines hangars evolved from a major study sponsored by six prominent airlines entitled, "Maintenance Environments for Boeing 747's and Boeing SST's." This report, prepared by Lev Zetlin Associates, Inc., Consulting Engineers, developed building systems for all combinations of aircraft and maintenance operations, considering both conventional and new material applications. These studies and the American Airlines project have indicated the potential of developing free form primary steel structures with light-gage steel. The American Airlines project is a solution which meets the criteria of economy, flexibility for future change in an ever changing industry, lightweight, functionality and aesthetic appearance in an age where attractiveness of large industrial type facilities is becoming an important factor in our environment (see Figure 1).

II. THE HANGAR BUILDING SYSTEM

In order to accommodate as many present-day aircraft as possible and at the same time be capable of housing four Boeing 747's or six McDonnell-Douglas DC-10's and, in addition, be flexible enough in plan to accept the next, as yet unknown, generation of aircraft, a double cantilever configuration was selected. The overall dimensions of the facility shown in Figure 2 are 450 feet along the door sides of the building and 560 feet at the end wall. The central core area is 100 feet wide and 450 feet long. The hangar area is covered by a 230-foot cantilever on each side of the core. Figure 3 shows a cross-section and front view of the structure. The geometry of the roof structure is based upon structural and functional requirements. The following criteria are the guide lines by which the roof system was conceived:

1. The roof system should be both economical and lightweight.
2. The slope of the top surface of the roof structure should conform to the Federal Aviation Administration requirement for Instrument Landing Systems (ILS) clearance.
3. The soffit of the roof should be horizontal to allow for uniform clear height within the hangar. This allows tail-in and nose-in capability and also facilitates overhead bridge crane operation.
4. The line of the roof structure should be level at the tip of the cantilever in order to simplify the door configuration.
5. There should be no columns nor permanent supports within the hangar space or around the hangar perimeter to allow for flexibility in future expansion of the facility.
6. The shape of the roof should be such that the vertical tail of the aircraft can protrude up into the roof area when jacked to remove gears.
7. The shape of the roof should be such that draft curtains to contain and control the build-up of heat can be eliminated. A folded shape accomplishes this.
8. The plan of the building and the support system of the roof should allow for an optimization of the required area per plane and for future flexibility.
9. The structural system should be such that it could be utilized at any geographical site in the world. Snow, thermal, seismic, wind and hurricane loadings should be resisted by the system.

Because of the magnitude of the structure, economy was achieved by evolving a system which embodies mass-production and pre-manufacturing techniques but uses conventional, readily available materials. The roof system developed is comprised of 16 basic structural modules; eight modules on each side of the central core (see Figures 2 and 3). These modular 56-feet by 230-feet roof elements are comprised of two 28-feet by 230-feet light-gage hyperbolic paraboloids. Each roof module (hypar) consists of a ridge member, two valley members, edge members and the warped hyperbolic paraboloids. Figures 4 and 5 show the typical roof module. The ridge and valley members are hot-rolled A-572 steel. The material selected for the hyperbolic paraboloids was cold-formed light-gage steel decking consisting of a flat, 13-gage sheet, 26 inches wide with two 9-inch wide by 7½-inch deep, 18-gage hat sections, resistance welded to the flat sheet. A typical cross-section of the deck is shown in Figure 6.

[1]President, Lev Zetlin Associates, Inc., New York, New York

[2]Associate, Lev Zetlin Associates, Inc., New York, New York

[3]Vice President for Research, ENVIRONSPACE Research and Technology Corp., Affiliate of Lev Zetlin Associates, Inc., New York, New York

FIGURE 1

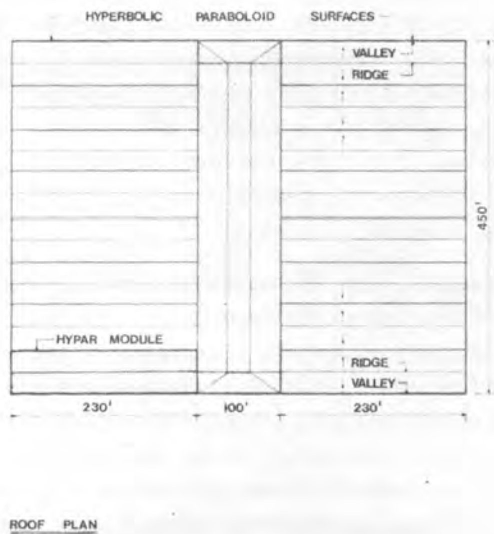

FIGURE 2

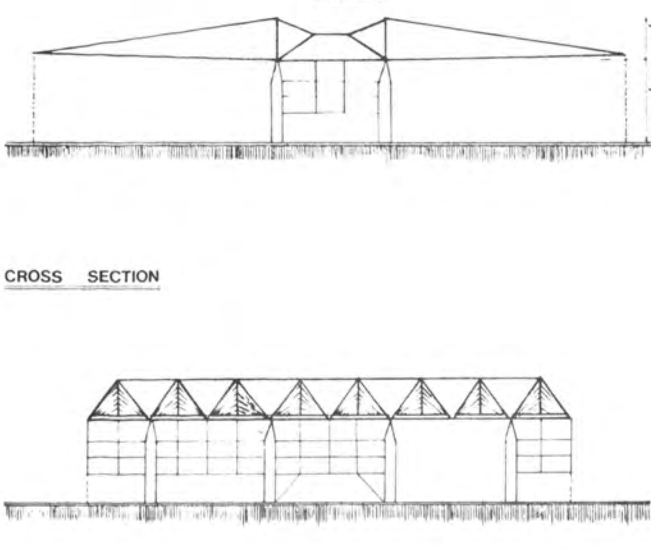

FIGURE 3

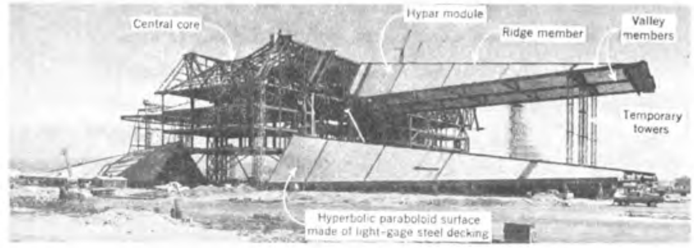

FIGURE 4

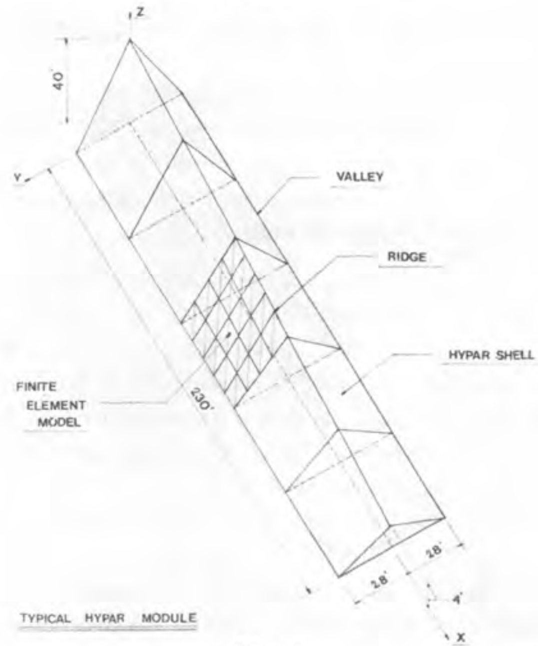

FIGURE 5

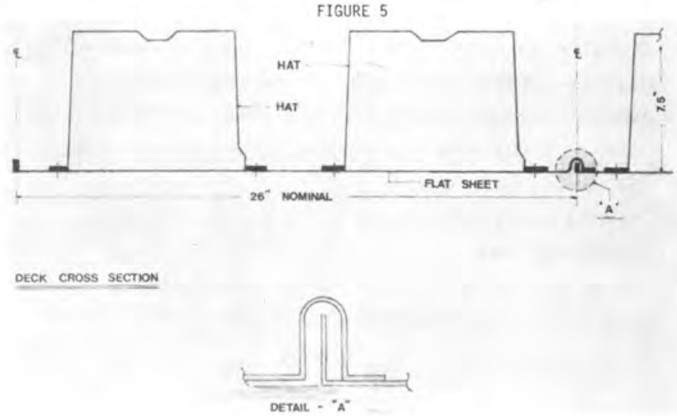

FIGURE 6

The entire hypar surface is generated by the same deck elements being placed between the ridge and valleys. Intermittent seam welds between the decks maintain the shell shear strength, and connect the shell to the ridge, valley and edge members around the perimeter of the deck panel. To enable the structural system to be feasible in any area of the world, a system of prestressing cables is incorporated into the shell structure. The structural strand cables induce a prestress in the shell which makes the system readily adaptable to any geographical site (see Figure 7).

III. STRUCTURAL TECHNOLOGY

The underlying concept behind the development of the system is that in normal construction, the roofing deck is structurally inert as far as contributing to the primary structural system. The deck usually spans between purlins or trusses and only serves to form the roof surface. Therefore, in the hypar concept, the key to economy is the fact that the deck serves a dual purpose; primary structure and roof surface. Hyperbolic paraboloids are possessed with a geometry that enables them to carry applied loads primarily in a state of shear. Light-gage steel decking is endowed with a high shear capacity to weight ratio. Thus, the use of a light-gage hyperbolic paraboloid is natural. According to the membrane theory of shells, a hyperbolic paraboloid carries uniformly distributed loads in such a manner that the state of stress is uniform throughout the shell. As a result, the shell can be of uniform cross-section and thus lends itself to mass production.

Because the loading on the roof structure is a combination of surface dead load of the deck and roofing, edge loadings due to ridge and valley weights, wind and seismic forces, live loads and concentrated crane loads, the membrane theory of shells does not directly apply. In order to obtain an accurate solution for the deformations of the structure and the exact distribution of the shear stresses throughout the shell, finite element techniques were utilized. The structure was subdivided into elements as shown in Figure 5. Each element accounted for all the stress resultants within the shell. Membrane forces and bending and torsional moments within the deck were included in the analysis. The structure was idealized into a structural assembly of 400 finite triangular elements and 127 uni-dimensional space frame members. Each solution for the different loading conditions required the solution of 2,075 linear simultaneous equations. Two different finite element approaches were utilized. One approach considered each element to be a plate element while the other treated each element as a shell surface. Both methods yielded close comparison.

As mentioned previously, the membrane theory state of shear is uniform and is governed by the following equation:

$$N_{xy} = \frac{wab}{2c} \qquad (1)$$

Where N_{xy} = shear resultant, w = uniform load, a and b are the plan dimensions of the shell, and c equals the rise of the shell. Considering the total dead and live load as a uniform load of 40 psf. Equation (1) gives N_{xy} = 3,200 plf. The actual shear stress distribution as obtained by finite element methods is plotted in Figure 8 for dead load plus live load plus cable prestress. It can be seen that the actual distribution is quite uniform at the center nodes. The distribution, however, varies slightly in the vicinity of the ridge and valley.

The close comparison to the uniform maximum shear of membrane theory is made possible by the male-female joint between deck elements (see Detail A in Figure 6). This joint acts as a bellows or release when tensile or compressive forces act perpendicular to it. This offers a very advantageous effect. If no release was present, i.e., the joint was a lap joint, the stresses in the deck in the vicinity of the ridge and valley would be very high due to strain compatibility with the ridge and valley members. The membrane theory does not consider strain compatibility of boundary members. The releases reduce the tensile and compressive strains and stresses to very low levels. In order to account for this effect in the finite element analysis the stress resultants were made zero in the X-direction. Studies using the computer were made to compare the effect of the stress release mechanism. The results for the case with no stress releases were considerably different than the uniform results obtained for the released case, and contained very high tensile and compressive forces in the deck. If the stress releases were not introduced, the system would not have been feasible.

The maximum shear resultant encountered due to dead load, live load and cable prestress was approximately 3,600 pounds per foot. Using the AISI light-gage design recommended load factors of 2.2 on dead load and 3.0 on live load, the ultimate strength required for the deck is 10,000 pounds per foot. Computations indicated that the 13-gage, 18-gage deck would successfully carry the 10,000 pounds per foot shear. However, since shear values of this magnitude had never been tested to date and because the calculation of the buckling load of the shell was inconclusive, full scale testing of a portion of the roof system was specified, as described in Section IV.

The magnitude of the localized bending moments in the ridge and valley members was analysed through the use of the finite element approach. Membrane theory does not account for the flexure of the edge members. Figure 9 shows the distribution of these bending moments. The existence of these bending moments near the tip of the cantilever dictated that the depth of the ridge and valley members be increased near the tip to 36 inches. This additional depth substantially reduces the localized flexural deformation near the tip and maintains the curvature of the deck which is sensitive to local deflection in the flatter portions of the shell. The strength of the shell is proportional to its curvature. The ridge and valley members are built-up steel members comprised of 50,000 psi yield material. These members, which are proportioned to carry axial load and the localized bending moments, are 24 inches deep near the core area and 36 inches deep at the tip.

In order to further reduce the localized distortions in the vicinity of the tip of the cantilever, the rise of the shell at the tip was set at 4 feet. This rise allowed the inclusion of a stiffening truss to tie all the roof modules together and eliminate relative rotation of the modules due to wind uplift and crane loads.

A second computer analysis using finite element techniques was undertaken to verify the behavior of one quadrant of roof. Unit loads were applied at regular intervals both horizontally and vertically to develop influence surfaces for the structure. Dead load, live load, wind, seismic and crane loads were considered. Particular emphasis was placed upon the crane loads which result in the largest concentrated loads. The results of this four module analysis, which utilized a coarser finite element pattern, were compared with the results of model tests.

Because of the unique nature of the structure and the advantages of optimizing the prototypical design, a program of structural model testing was undertaken. This program included a static wind model, an aeroelastic wind model, a large scale structural model of a single hypar module and a smaller scale structural model of a quadrant of four hypar modules (see References 1 and 2).

The series of cables varying in diameter from ½ inch to 1 inch which are incorporated into the system, act as a prestressing device which relieves the shear resultants in the deck by as much as 20%. Because of the limitations on the capacity of the deck and due to the prototypical nature of the structure, the cables are necessary to make the system universally applicable. The first two structures built in California are designed for a live load of 12 psf. When the system is used in colder climates where snow loading is of importance, the deck configuration could remain the same, but the magnitude of the load carried by cables would increase.

IV. STABILITY ANALYSIS OF DECK

Various approaches to analysing the structural stability of the hypar deck were investigated. To the knowledge of the authors, there is no theoretical analysis presently available which directly applies to calculating the buckling characteristics of the roof shell. The shell can be classified as a hyperbolic paraboloid with orthotropic properties. It has zero bending rigidity along discrete lines orthogonal to the shells' direction of maximum bending rigidity and has torsional rigidity defined on finite sections bounded by these same lines. In addition, the shell has negligible in-plane stiffness in one direction. That is to say, that the hat sections cause the primary bending rigidity of the shell to be in the Y direction (parallel to the hats); in the X direction, the flat sheet of the deck has its bending rigidity interrupted by the bellows joint, which also prevents the deck from having a tensile or compressive capacity in the X direction. Each individual cell formed by the hats over the flat sheet, develops the discrete torsional rigidities, linked by either the bellows joint or the 13-gage flat sheet. Most of the methods of analysis neglected torsional rigidity of the hats as relationships between the discrete rigidities and the rigidity to be used in a continuous analysis was not apparent. What was apparent, however, was the significant effect these rigidities have upon the buckling strength of the shell. Of the numerous approaches taken to bound the buckling load of the shell, a few of the most promising, with comparisons to test results are described below.

One approach modified the classical buckling formulas for isotropic hyperbolic paraboloid shells based on the relationship between the analysis of isotropic and orthotropic flat plates subjected to pure shear. The hat stiffeners on the shell are sufficiently close to permit analogy to orthotropic plate and shell theories based on continuum mechanics. The buckling of an orthotropic plate subjected to pure shear (Figure 10) is governed by the differential equation:

$$D_1 \frac{\partial^4 w}{\partial x^4} + 2D_3 \frac{\partial^4 w}{\partial x^2 \partial y^2} + D_2 \frac{\partial^4 w}{\partial y^4} = 2N_{xy} \frac{\partial^2 w}{\partial x \partial y} \qquad (1)$$

where

$$D_1 = \frac{EI_x}{(1-\nu_x \nu_y)} \qquad D_2 = \frac{EI_y}{(1-\nu_x \nu_y)} \qquad (2,3)$$

$$D_3 = \tfrac{1}{2}(\nu_x D_2 + \nu_y D_1) + 2(GI)_{xy} \qquad (4)$$

w = Deflection	E = Modulus of Elasticity
N_{xy} = Shear Resultant	G = Shear Modulus
I = Moment of Inertia	ν = Poisson's Ratio

For an isotropic plate, $\nu_x = \nu_y$ and $2(GI)_{xy} = D(1-\nu)$, giving $D_1 = D_2 = D_3 = EI/(1-\nu^2)$. The solution for the critical shear resultant of a simple supported isotropic plate with large a/b is

$$N'_{xy} = 5.35 \frac{\pi^2 D}{b^2} \qquad (5)$$

The critical shear for a simple supported orthotropic plate is:

$$N_{xy} = \frac{4K \sqrt{D_2 D_3}}{b^2}, \qquad \theta < 1 \qquad (6)$$

$$= \frac{4K \sqrt[4]{D_1 D_2^3}}{b^2}, \qquad \theta > 1 \qquad (7)$$

where:

$$\theta = \frac{\sqrt{D_1 D_2}}{D_3} \qquad (8)$$

Assuming $D_1 = 0$, because of the bellows joint, then $\theta = 0$, and $K = 11.7$ for large a/b (see Reference 3). This yields

$$N_{xy} = 46.8 \frac{\sqrt{D_2 D_3}}{b^2} \qquad (9)$$

Therefore the relationship between the orthotropic and isotropic case becomes

$$N_{xy} = 0.885 \frac{\sqrt{D_2 D_3}}{D} N'_{xy} \qquad (10)$$

Reissner's equation (see Reference 4) for the critical shear resultant for an isotropic hyperbolic paraboloid shell of thickness h, with simply supported edges and subjected to uniform loading on its projected surface may be expressed as

$$N_{xy} = 2 \frac{c}{ab} \sqrt{EhD} \qquad (11)$$

As above, substitute

$$D = 0.885 \sqrt{D_2 D_3} \qquad (12)$$

giving for the hypar shell

$$N_{xy} = 1.88 \frac{c}{ab} \sqrt{Eh \sqrt{D_2 D_3}} \qquad (13)$$

Both Equations 11 and 13 indicate the dependence of the buckling load on both the bending rigidity and the thickness associated with the shell, as well as the curvature. If we eliminate h by further substitution in Equation 13 of

$$Eh^3/12(1-\nu^2) = 0.885\sqrt{D_2D_3} \quad (14)$$

we obtain in Equation 13 the effect of an equivalent thickness associated with Equation 14. Equation 13, therefore, becomes

$$N_{xy} = 2.86\,\frac{c}{ab}\left[ED_2D_3\sqrt{1-\nu^2}\right]^{1/3} \quad (15)$$

Various assumptions are possible within the above approach. The most conservative lower bound solution was obtained with Equation 13, taking h as the thickness of the 13-gage flat sheet; D_3 as the torsional rigidity of the flat sheet only ($D_3 = Eh^3/12(1-\nu^2)$); and D_2 as the bending rigidity in the direction of the hats. This yielded N_{xy} = 11 kips/ft. This was very conservative as it did not account for the torsional stiffness of the hats.

The upper limit value of torsional rigidity was calculated for the deck hats, neglecting the flexibility of the 13-gage flat sections between the hats. This was done by calculating $(GI)_{xy}$ and thus, D , from the expression for torsional moment, M_{xy}, from orthotropic plate theory,

$$M_{xy} = 2(GI)_{xy}\,\frac{\partial^2 w}{\partial x \partial y}$$

M_{xy} is calculated from the torque applied to an open section consisting of the hat closed by the 13-gage plate sheet and $\partial^2 w/\partial x\partial y$ is the angle of twist per unit length of the open section. This analysis yielded D_3 in the order of 10^7 in-pounds as compared to 2,000 for D_3 based on the isotropic flat 13-gage sheet only. Based on observations of forces and deflections associated with twisting the deck during preliminary tests, D_3 was calculated as 10^6in-pounds. Using this value of D_3 in Equation 13 yielded N_{xy} = 52 kips/ft.

The analysis indicates the significance of the torsional rigidity upon the buckling strength of the shell in the absence of bending rigidity in the Y direction (D_2). Use of Equation 15 gives higher values as it incorporates the use of an effective thickness coupled to values of D.

It should be emphasized that the torsional stiffness of the hats has such a significant effect on the buckling strength because of D_1 being assumed zero. Studies of orthotropic plate theories indicate that given any two significant rigidities from D_1, D_2, and D_3, and one is assumed negligible, the bringing of the small rigidity to the order of magnitude of the other two, does not significantly effect the buckling load. In certain ranges of parameters, this effect is also true for an orthotropic shell.

Another approach to calculating the buckling load of the hypar shell was based on the work of Dr. Richard Muskat's Doctoral Thesis at Cornell University on the buckling of orthotropic corrugated light gage hyperbolic paraboloids (Reference 5). Muskat develops the critical buckling shear as:

$$N_{xy} = 2\,\frac{c}{ab}\sqrt{EhD}\sqrt{f}$$

This form of the equation ignores pre-critical deflections such as those due to flexible edge members which Muskat shows to be negligible. The form of the equation indicates that it is Reissner's equation for an isotropic hypar modified by $\sqrt{f}$ which accounts for orthotropicity, where

$$f = \sqrt{(R_4 + R_5 + R_6)/(R_1 + R_2 + R_3)}$$

and where for a single layer shell

$R_1 = \Psi(1-\nu^2)/(\beta\Psi-\gamma^2)$

$R_2 = -\left[2\gamma(1-\nu^2)/(\beta\Psi-\gamma^2) - (1-\nu^2)/\rho\right]$

$R_3 = (\beta/\Psi)R_1$

$R_4 = \beta$

$R_5 = 2\left[\gamma + 2\rho\right]$

$R_6 = \Psi$

where

$\beta = D_x/D$

$\Psi = D_y/D$

$\gamma = D_1/D$

$\rho = D_{xy}/D$

Note that correlating with the previous equations,

$D_1 = D_x, \quad D_2 = D_y, \quad D_3 = D_1 + 2D_{xy}$

The form of this solution, however, does not permit D_x to be taken as zero. Therefore, D_x was calculated as the bending rigidity of a corrugated sheet in the weak direction, assuming the bellows joint as typical of the corrugations. With this approach, and using the previous value for torsional rigidity based on the experimental observations, the critical buckling shear was calculated as N_{xy} = 57 kips/ft.

Numerous other approaches were taken, and assumptions made in studying the buckling characteristics of the shell. Although the above two approaches may seem to have similar results, one must recognize their sensitivity to certain assumptions. For example, the previous analysis is very sensitive to the value of D_x for the particular range of parameters involved. These analyses are presented here as illustrations of the practical approaches possible in bounding the value of the buckling load of a hypar deck. They should not be misconstrued as a directly applicable design analysis approach for use by the practicing engineer, without confirmation by testing.

A full-scale test was conducted to confirm the buckling integrity of the deck as well as to test the method of welding. A 30-foot by 50-foot panel warped to the same curvature as the prototype was subjected to normal loads. This test confirmed the buckling load of the deck to be in excess of the required shear value of 10,000 pounds per linear foot (see Reference 2). The test conducted, simulated the hypar action in the protoype which was confirmed by edge member deflections, as well as strain gage readings. The test was conservative in that the test support system caused the test hypar to have a higher ratio of bending action to shell action. All practical light-gage hyperbolic paraboloid shells will experience a certain amount of local bending in the shell compared to its primary shell action. The smaller the ratio of bending action to shell action, the stronger the structure.

The internal valley members were restrained from Euler buckling continuously by the deck. The valley members at the end of the building were partially restrained by the deck and contained additional stiffness and support to resist Euler buckling. Due to the restraint of the deck, the critical mode of buckling for the internal valleys was torsional buckling. Connections were designed which permitted the bending resistance of the hypar deck to be used in applying a system of discrete rotational constraints which prevent the torsional buckling of the valley members.

V. FABRICATION OF THE DECK

The deck was fabricated by resistance welding the hats to the flat sheet. The resistance welds were specified at a spacing of 4½ inches center to center, which was the same spacing used in the large scale test. The deck was actually fabricated with a resistance weld spacing of 2¼ inches in order to simplify quality control.

A unique quality control program was developed to insure the reliability of the resistance welds, and all the seam and edge welds, as the deck was the primary structure of the roof system. The program consisted of periodic random tests on sections of deck and both visual inspections and random X-ray testing as well as periodic inspections of the resistance welding machine. The quality control program proved that resistance welding techniques could be developed to insure reliable spot weld connections on light-gage deck. For example, numerous random samples of deck, 10 feet long and containing about 240 spot welds, were tested by prying the hats completely off of the flat sheet. The spot weld was acceptable if it pulled a nugget out of the parent material at failure. The quality control program led too many of these samples having none of the 240 spot welds fail.

Stick and mig welding was used for the seam welds and end welds which were 3 inches long and placed every 6 inches. The quality control program also enabled one to have the highest level of confidence in these welds. In addition, fatigue tests were conducted to insure the life of these welds under conditions of repeated loading due to wind and crane loads.

The hypars were fabricated by placing either individual 26-inch wide panels, or three pre-welded panels, in place between the ridge and valley members where they were manually warped into place. All of the hypar modules were fabricated on the ground and then lifted into place and bolted to the core structure. When the shores were removed, the maximum deflection under dead load recorded at the tips of the 230-foot cantilevered modules, was only 7 inches.

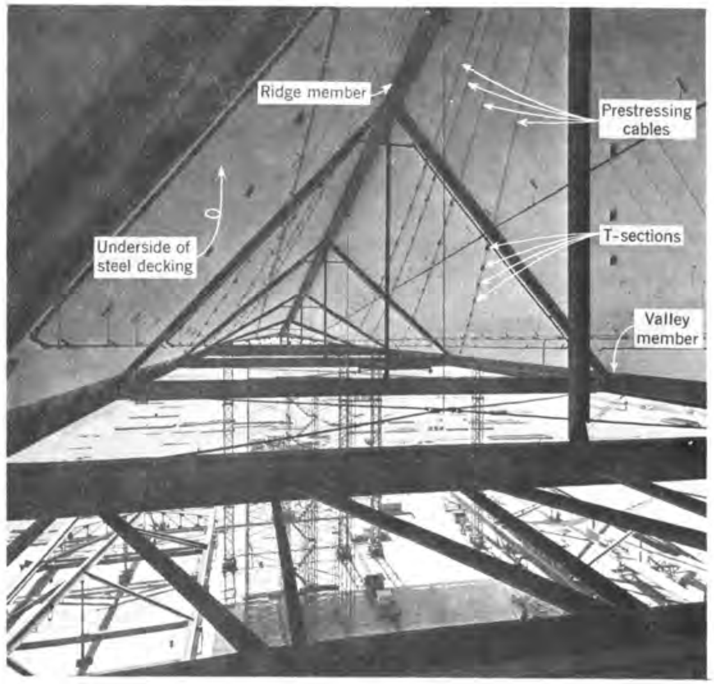

FIGURE 7

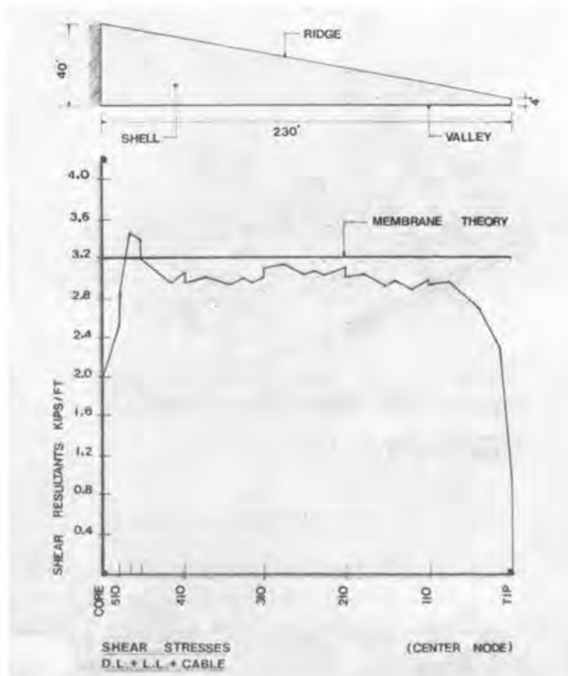

FIGURE 8

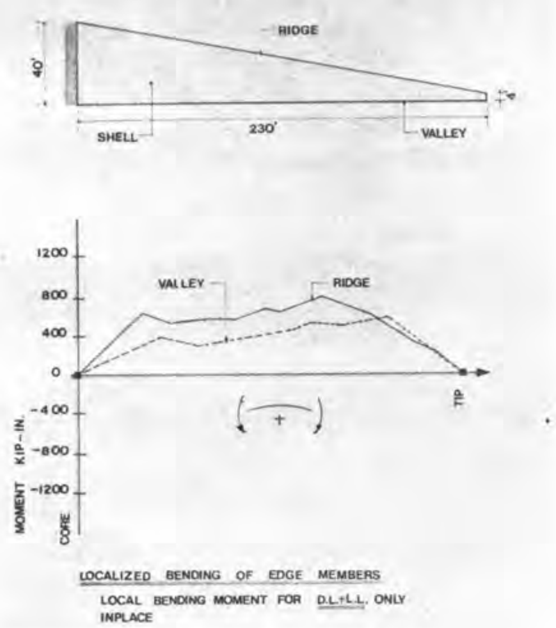

FIGURE 9

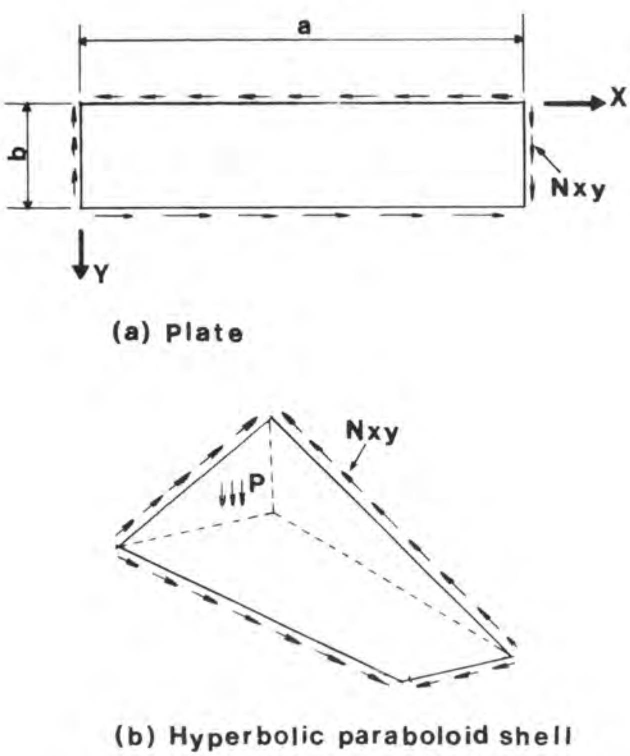

FIGURE 10

VI. CONCLUSIONS

This project has illustrated the potential of light-gage steel for use as primary structure for constructing economical large span buildings. Methods of design have been developed which advance the use of light-gage steel for free form structures. Methods of analysis and testing have been applied which permit the design of large light-gage hyperbolic paraboloids. The project has demonstrated that quality control procedures can significantly increase the structural reliability of resistance and fusion welds on light-gage steel sheets. The potential of industrializing large building systems fabricated from light-gage steel components has been demonstrated.

VII. REFERENCES

1. Zetlin, L. and Thornton, C., "World's Largest Light-Gage Steel Folded Hyperbolic Paraboloidal Shell Roof Structure", International Association of Shell Structures - Symposium Wien, 1970.

2. Moreno, A., Thelen, J., Thornton, C., Tomasetti, R., Waddington, W., "Static and Dynamic Model Studies of American Airlines' B-747 Hangar Roof Structure", ASCE National Structural Engineering Meeting, April 1971.

3. Timoshenko, S., and Gere, J., "Buckling of Thin Plates", Theory of Elastic Stability, McGraw-Hill Book Company, Inc., New York, 1961.

4. Reissner, E., "On Some Aspects of the Theory of Thin Elastic Shells", Boston Society of Civil Engineers.

5. Muskat, R., "Doctoral Thesis on Buckling of Orthotropic Hyperbolic Paraboloids", Cornell University, 1969.

VIII. ACKNOWLEDGEMENTS

The American Airlines' Superbay Hangars were designed by the joint venture of Lev Zetlin Associates, Inc., Structural Engineers, and Conklin and Rossant, Architects, both of New York City. Model studies were performed by Wiss-Janney-Elstner and Associates, Northbrook, Illinois. The full scale testing was performed by Inland-Ryerson Construction Products, Milwaukee, Wisconsin.